

# Adding Compliant Joints and Segmented Foot to Bio-inspired Below-knee Exoskeleton

Jinying Zhu, Qining Wang, Yan Huang and Long Wang

**Abstract**—This paper presents a bio-inspired below-knee exoskeleton to assist human walking. Different from the passive orthotic devices, the proposed exoskeleton includes powered compliant ankle and toe joints, which can output sufficient power to help the one with exoskeleton relearn normal walking gaits. We first propose a passivity-based dynamic bipedal model to analyze the effects of segmented foot and compliant joints on energetic efficiency and stability of bipedal walking. Starting from the results of theoretical analysis, we construct a below-knee exoskeleton prototype with ankle and toe joints driven by two series-elastic actuators. Experimental results validate the effectiveness of the proposed exoskeleton.

## I. INTRODUCTION

Although exoskeleton was invented several decades ago, the development of the exoskeleton is not as fast as people expect [1]. In the late 1960s, the first exoskeleton (Hardiman) was built [2], which can well increase the strength of the arms, but not solve the problems with lower limb components. Recently, [3] developed the Berkeley Lower Extremity Exoskeleton (BLEEX). It includes powered hip, knee and ankle joints, which are actuated by bidirectional linear hydraulic cylinders mounted in a triangular configuration. In addition, since the wearer's foot is connected with the exoskeleton by a stiff metal plate, the wearer's feet are not allowed to bend, which may affect the walking gait. Then, [4] designed articulated lower extremity orthoses with pneumatic muscle actuators to provide additional power to the joints of the lower extremity during gait. Though the hydraulic or the pneumatic actuator is lightweight and capable of generating high forces and inherently compliant, its control difficulties, large size and noise restrain the development of the powered exoskeleton. Hybrid Assistive Leg (HAL) has been developed for both performance-augmenting and rehabilitative purposes [5]. The exoskeleton includes powered hip and knee joints actuated by DC motor. However, there is no powered toe joint in the existing exoskeleton systems.

To evaluate the effects of multi-segmented foot structures on human normal walking, increasing studies on segmented foot models have been proposed [6]. Different from the traditional methods that represent the foot as a single rigid bar, multi-segmented foot models have been studied for investigations of clinical and research applications [7], adolescent gaits [8] and pediatric gaits [9]. The results show

that the segmented foot with toe joint has several advantages compared to the single rigid foot in the following aspects: walking step, walking speed, range of joint angle and the changing of angle velocity and joint energy-output.

Inspired by the biological studies, in this paper, we develop a below-knee exoskeleton (EXO-PANTOE 1) with compliant joints and segmented foot, which is adapted from our recent powered below-knee prosthesis (PANTOE 1) with active toe joint [10]. To analyze the effects of segmented foot and compliant joints on energetic efficiency and stability of bipedal walking, we first propose a passivity-based dynamic bipedal model which shows resemblance to human normal walking. Starting from the theoretical analysis, we introduce segmented foot with toe joint to the exoskeleton prototype. Both the ankle and toe joints are driven by two series-elastic actuators (SEA), which not only provide enough torque, but also tolerance shocks and store energy during walking. Preliminary studies of sensory based feedback control method are carried out to improve the movement of the proposed exoskeleton. Experiments show the wearing results of the proposed exoskeleton by real human.

The rest of the paper is organized as follows. Section II presents the passivity-based bipedal model and related analysis. Section III proposes the development and control of the below-knee exoskeleton prototype. Section IV shows the experimental results. We conclude in Section V.

## II. ADDING COMPLIANT JOINTS AND SEGMENTED FEET

### A. Human Normal Walking Gaits

Human walking is a cyclic pattern of bodily movements that is repeated over and over, step after step. Every gait cycle starts with heel-strike (HS) when the heel initially touched the ground and ends with the next HS of the same leg. As shown in Fig. 1, each cycle can be divided into two main phases: stance phase and swing phase [11]. The stance phase begins at the moment of HS and ends at the moment of toe-off (TO) when the forefoot pushes off the ground. The swing phase begins at the moment TO and ends at the next HS. The stance phase takes up 60% of the gait cycle and includes four subphases: 1) HS to Foot-Flat (FF); 2) FF to Midstance (MS); 3) MS to Heel-Off (HO); 4) HO to TO.

### B. Passivity-based Bipedal Model

To further investigate the effects of compliant joints and segmented feet on dynamic bipedal walking which can guide the design and control of efficient and effective below-knee exoskeleton, in this section, we propose a passivity-based dynamic bipedal walking model that is more close to human

This work was supported by the National Natural Science Foundation of China (No. 61005082, 61020106005), Doctoral Fund of Ministry of Education of China (No. 20100001120005) and the 985 Project of Peking University (No. 3J0865600)

The authors are the Intelligent Control Laboratory, College of Engineering, Peking University, Beijing 100871, China.

Email: Q. Wang (qiningwang@pku.edu.cn)

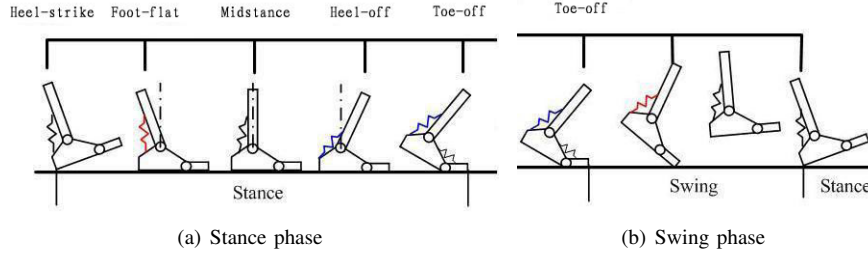


Fig. 1. One typical gait cycle. Each cycle includes two main subdivisions: (a) stance phase, (b) swing phase. The four important instant in every cycle are heel-strike (HS), foot-flat (FF), heel-off (HO) and toe-off (TO).

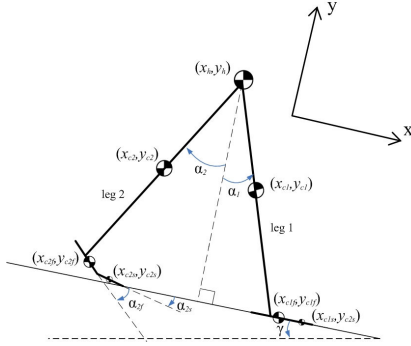


Fig. 2. Passivity-based dynamic bipedal walking model with flat segmented feet and compliant ankle joints.

beings. Passive dynamic walking [12] has been developed as a possible explanation for the efficiency of the human gait. We add compliant ankle joints and flat segmented feet with compliant toe joints to the passivity-based model. As shown in Fig. 2, the two-dimensional model consists of two rigid legs interconnected individually through a hinge. Each leg contains segmented foot. The mass of the walker is divided into several point masses: hip mass, leg masses, masses of foot without toe, toe masses. Each point mass is placed at the center of corresponding stick. Torsional springs are mounted on both ankle joints and toe joints to represents joint stiffness. To simplify the motion, we have several assumptions, including that legs suffering no flexible deformation, hip joint with no damping or friction, the friction between walker and ground is enough, thus the flat feet do not deform or slip, and strike are modeled as an instantaneous, fully inelastic impact where no slip and no bounce occurs. The passive walker travels on a flat slope with a small downhill angle.

The process of push-off is dissipated into foot rotation around toe joint and around toe tip, which is the main difference between the passive walking models with rigid flat feet and with segmented flat feet. The toe and foot are restricted into a straight line during the swing phase. When the flat foot strikes the ground, there are two impulses, "heel-strike" and "foot-strike", representative of the initial impact of the heel and the following impact as the whole foot contacts the ground. After foot-strike, the stance leg and the swing leg will be swapped and another walking cycle will begin. The passive walking is restricted to stop in two cases,

including falling down, running. We deem that the walker falls down if the angle of either leg exceeds the normal range. And the model is considered to running when the stance leg lifts up while the swing foot has no contact with ground. And foot-scuffing at mid-stance is neglected since the model has no knee joints.

We suppose that the x-axis is along the slope while the y-axis is orthogonal to the slope upwards. The configuration of the walker is defined by the coordinates of the point mass on hip joint and six angles (swing angles between vertical coordinates and each leg, foot angles between horizontal coordinates and each foot, toe angles between horizontal coordinates and each toe), which can be arranged in a generalized vector  $q = (x_h, y_h, \alpha_1, \alpha_2, \alpha_{1f}, \alpha_{2f}, \alpha_{1t}, \alpha_{2t})^T$  (see Fig. 2). The positive direction of all the angles are counter-clockwise.

### C. Walking Dynamics

The model can be defined by the rectangular coordinates  $x$ , which can be described by the x-coordinate and y-coordinate of the mass points and the corresponding angles (suppose leg 1 is the stance leg):

$$x = [x_h, y_h, x_{c1}, y_{c1}, \theta_1, x_{c2}, y_{c2}, \theta_2, x_{c1f}, y_{c1f}, \theta_{1f}, x_{c2f}, y_{c2f}, \theta_{2f}, x_{c1s}, y_{c1s}, \theta_{1s}, x_{c2s}, y_{c2s}, \theta_{2s}]^T \quad (1)$$

The walker can also be described by the generalized coordinates  $q$  as mentioned before:

$$q = [x_h, y_h, \alpha_1, \alpha_2, \alpha_{1f}, \alpha_{2f}, \alpha_{1t}, \alpha_{2t}]^T \quad (2)$$

We defined matrix  $T$  as follows:

$$T = \frac{dq}{dx} \quad (3)$$

Thus  $T$  transfers the independent generalized coordinates  $\dot{q}$  into the velocities of the rectangular coordinates  $\dot{x}$ . The mass matrix in rectangular coordinate  $x$  is defined as:

$$M = \text{diag}(m_h, m_h, m_l, m_l, I_l, m_l, m_l, I_l, m_f - m_s, m_f - m_s, I_f, m_f - m_s, m_f - m_s, I_f, m_s, m_s, I_s, m_s, m_s, I_s) \quad (4)$$

Denote  $F$  as the active external force vector in rectangular coordinates. The constraint function is marked as  $\xi(q)$ , which is used to maintain foot contact with ground and detect impacts. Note that  $\xi(q)$  in different walking phases may be different since the contact conditions change.

We can obtain the Equation of Motion (EoM) by Lagrange's equation of the first kind:

$$M_q \ddot{q} = F_q + \Phi^T F_c \quad (5)$$

where  $F_c$  is the contact force acted on the walker by the ground to meet the constraint of the stance foot.

$$\xi(q) = 0 \quad (6)$$

where  $\Phi = \frac{\partial \xi}{\partial q}$ .  $M_q$  is the mass matrix in the generalized coordinates:

$$M_q = T^T M T \quad (7)$$

$F_q$  is the active external force in the generalized coordinates:

$$F_q = T^T F - T^T M \frac{\partial T}{\partial q} \dot{q} \quad (8)$$

Equation (6) can be transformed to the followed equation:

$$\Phi \ddot{q} = -\frac{\partial(\Phi \dot{q})}{\partial q} \dot{q} \quad (9)$$

Then the EoM in matrix format can be obtained from Equation (5) and Equation (9):

$$\begin{bmatrix} M_q & -\Phi^T \\ \Phi & 0 \end{bmatrix} \begin{bmatrix} \ddot{q} \\ F_c \end{bmatrix} = \begin{bmatrix} F_q \\ -\frac{\partial(\Phi \dot{q})}{\partial q} \dot{q} \end{bmatrix} \quad (10)$$

The equation of strike moment can be obtained by integration of Equation (5):

$$M_q \dot{q}^+ = M_q \dot{q}^- + \Phi^T I_c \quad (11)$$

where  $\dot{q}^+$  and  $\dot{q}^-$  are the velocities of generalized coordinates after and before the strike, respectively. Here,  $I_c$  is the impulse acted on the walker which is defined as follows:

$$I_c = \lim_{t^- \rightarrow t^+} \int_{t^-}^{t^+} F_c dt \quad (12)$$

where  $I_c$  is the impulse acted on the walker by ground. Since the strike is modeled as a fully inelastic impact, the walker satisfies the constraint function  $\xi(q)$ . Thus the motion is constrained by the followed equation after the strike:

$$\frac{\partial \xi}{\partial q} \dot{q}^+ = 0 \quad (13)$$

Then the equation of strike in matrix format can be derived from Equation (11) and Equation (13):

$$\begin{bmatrix} M_q & -\Phi^T \\ \Phi & 0 \end{bmatrix} \begin{bmatrix} \dot{q}^+ \\ I_c \end{bmatrix} = \begin{bmatrix} M_q \dot{q}^- \\ 0 \end{bmatrix} \quad (14)$$

#### D. Effects of Compliant Joints and Segmented Feet

Based on the EoMs mentioned above, we analyze the effects of compliant ankles and toes on energetic efficiency and stability of dynamic bipedal walking. All mass and length are normalized by the leg mass and leg length respectively. The spring constants (stiffness of ankle joint and toe joint) are normalized by both the mass and the length of leg.

Energetic efficiency is an important gait characteristics. The energy consumption of passive dynamic based models is usually represented in the nondimensional form of

'specific resistance': energy consumption per kilogram mass per distance traveled per gravity [13], [14]. However, for passive walkers on a gentle slope, specific resistance is not a suitable measure of efficiency, since all walkers have the same specific resistance for a given slope [15]. Therefore, similar to [15], walking velocity is used as the measure of efficiency, such that "most efficient" is synonymous with "fastest".

The walking velocity of the rigid foot model (without toe joints) decreases monotonously as foot length or foot ratio (the ratio of distance between heel and ankle joint to distance between ankle joint and toe tip) grows (see Fig. 3(a)).

1) *Energetic Efficiency*: For the segmented foot model, the walker moves slower for longer foot according to the main tendency (see Fig. 3(b)). Walking velocity achieves the maximum value when foot ratio is near 0.3 for any fixed foot length. A peak appears at relative large foot length (larger than 0.2) and foot ratio near 0.3, which is similar to the foot structure of human beings [16]. The comparison of the two models shows that the walker with segmented feet moves slower than rigid foot model with small foot length, however, the velocity of segmented foot model is larger when the foot is long enough, especially when foot ratio is near 0.3. In another word, if the segmented foot ratio is close real human foot, the segmented foot model is more efficient than the rigid foot model.

2) *Walking Stability*: We evaluate adaptive walking of the model on uneven terrain to analyze the walking stability. Fig. 4 shows the relationship between the maximal allowable ground disturbance the walker can overcome and the foot ratio of rigid foot bipedal model.

The maximal allowable ground disturbance decreases monotonously as the foot ratio grows, which is similar to the tendency of curved surface of walking velocity. In the case of short hindfoot and long forefoot (foot ratio is 0.2), the walker can return to stable motion cycle after ground disturbance larger than 0.7 percent of leg length. However, the maximum disturbance the model can overcome decreases below 0.2 percent leg length when the lengths of hindfoot and forefoot are comparable (foot ratio is 0.8). The relationship between the maximal allowable ground disturbance and foot ratio of segmented foot model also shows a great resemblance to the walking velocity curved surface (Fig. 5 shows the results).

The maximal value is obtained when the foot ratio is 0.3. In that case the model can overcome the ground disturbance more than 0.6 percent leg length. The adaptability of segmented foot model decreases greatly if the foot ratio changes to other values. The results indicate that there exists a best foot structure of segmented foot model, which achieves both excellent adaptability and walking velocity.

From the analysis above, one can find that segmented foot models have comparable walking adaptability with rigid foot models in the case of suitable foot ratio. The walkers with segmented feet perform worse in other cases.

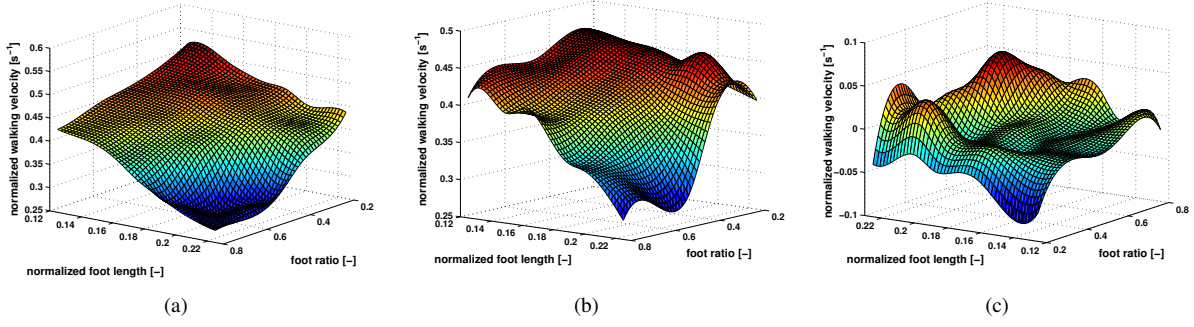


Fig. 3. Comparison of walking velocities of rigid foot model and segmented foot model. The curved surfaces are smooth processed based on the sample data. (a) Average walking velocity versus foot length and foot ratio for rigid flat-foot passive walking model. (b) Average walking velocity versus foot length and foot ratio for segmented flat-foot passive walking model. (c) The difference of walking velocity of the two models, obtained by (b) subtracts (a). Both walking velocity and foot length are normalized by leg length. Foot ratio is defined as the ratio of distance between heel and ankle joint to distance between ankle joint and toe tip.

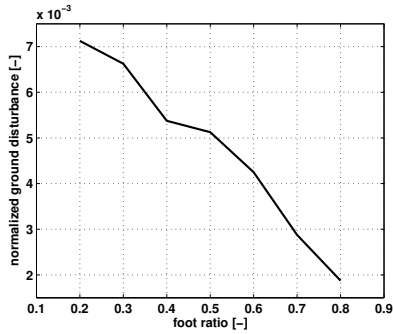


Fig. 4. Adaptability of the rigid foot model with different foot ratios. The normalized foot length is 0.1875. The ground disturbance is also normalized by leg length.

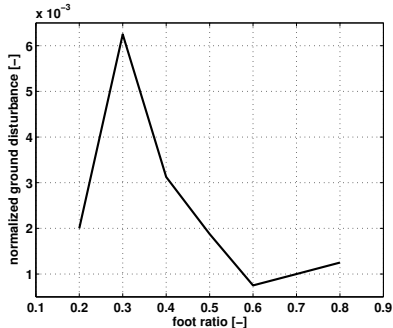


Fig. 5. Adaptability of the segmented foot model with different foot ratios. The normalized foot length is 0.1875. The ground disturbance is also normalized by leg length.

### III. EXOSKELETON PROTOTYPE

The theoretical analysis mentioned above indicates that segmented foot model with compliant joints is more complicated than rigid foot model in both foot structure and walking sequence. However, segmented foot models with foot structure close to human body show better walking performance (energetic efficiency and stability) compared with rigid-foot walking. Based on the results, we began the design of the exoskeleton prototype (EXO-PANTOE 1) with compliant joints and segmented foot.

EXO-PANTOE 1 is short for below-knee exoskeleton with powered ankle and toe joints. It is designed for a subject suffering from some ankle pathology. The information of the subject is shown in Table 1.

TABLE I  
INFORMATION OF THE SUBJECT.

Parameter	Value
length of the foot $L_1$	265mm
length of the forefoot $L_2$	79mm
level distance of the ankle joint from the end of the heel $L_3$	68mm
height of the ankle joint from the ground $H_1$	83mm
maximal plantar flexion angle of the ankle joint $\theta_p$	27°
maximal dorsiflexion angle of the ankle joint $\theta_d$	16°
maximal angle of the toe joint $\theta_t$	90°

As shown in Fig. 6, the basic architectures of EXO-PANTOE 1 are two SEAs, which are used to drive the ankle and toe joints respectively. Each SEA comprises of a

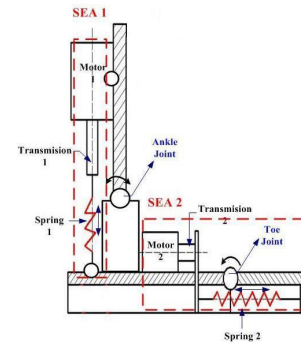


Fig. 6. Schematics diagram of EXO-PANTOE 1 with compliant joints and segmented foot. The two main components of the prosthesis are two SEAs, which are used to drive the ankle and toe joints respectively.

DC motor, a ball screw transmission and a spring structure. Because human toe joint only outputs net positive work at the moment TO, the toe joint is passive when bent, and active during TO. When toe joint is bent, Spring 2 will be extended to store energy. At the moment TO, Spring 2 will release the stored energy and Motor 2 will drive toe joint to rotate clockwise via Transmission 2 and Spring 2. Spring 2

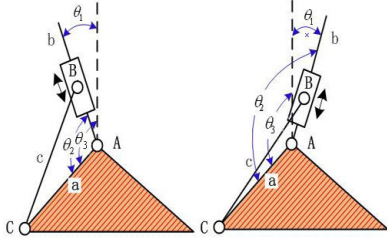


Fig. 7. The ankle joint can be simplified as a rotating guide-bar mechanism, of which the length of  $c$  can be modulated by SEA 1.

comprises four drawsprings set in parallel and the stiffness is  $180N/cm$ . Motor 2 used in the current design is a  $30W$  DC motor (with an angle encoder).

The ankle joint of EXO-PANTOE 1 can be simplified by a rotating guide-bar mechanism, shown in Fig.7. The rotating guide-bar mechanism comprises three bars ( $a$ ,  $b$  and  $c$ ), a slider, and three hinges ( $A$ ,  $B$  and  $C$ ). Hinge  $A$  is the ankle joint. Bars  $a$  and  $b$  are the foot and shank of EXO-PANTOE 1 respectively.  $c$  is a special bar, of which the length is determined by Spring 1.  $\theta_1$  is the angle of the ankle joint, which is used to control the movement of the ankle.  $\theta_1$  can be generated by the following equation:

$$\theta_1 = \arccos \frac{L_a^2 + L^2 - L_c^2}{2L_a L} - \theta_3 \quad (15)$$

Where,  $L$  is the distance between  $A$  and  $B$ , which is determined by Motor 1.  $L_a$  and  $L_c$  are the length of the bars  $a$  and  $c$  respectively.  $L_a$  and  $\theta_3$  can be calculated by  $L_3$  and  $H_2$  (shown in Table I):

$$\theta_3 = \pi - \arctan \frac{L_3}{H_1} \quad (16)$$

$$L_a = \sqrt{L_3^2 + H_1^2} \quad (17)$$

Based on the angle range of  $\theta_1$  from  $-16^\circ$  to  $27^\circ$ , we

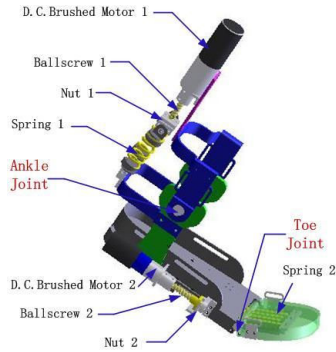


Fig. 8. The CAD model of the proposed exoskeleton with compliant joints and segmented foot.

designed SEA 1. Due to the demanding size in Table I, we construct Spring 1 with two springs placed together in parallel. The stiffness of Spring 1 is about  $300N/cm$ . The pitch of the ball screw Transmission 1 is  $4mm$ , then the nut is self-locking. Because the ankle needs to provide high power

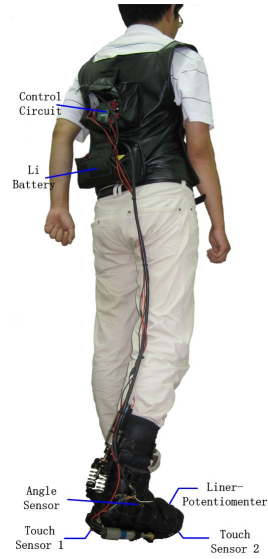


Fig. 9. The prototype of the proposed exoskeleton with compliant joints and segmented foot. It is made of aluminium-alloy. The weight is  $1.2\text{ kg}$  (not including the Li rechargeable battery about  $0.5\text{ kg}$ ), acceptable to the subject. The full angles of the ankle and the toe joints are  $45^\circ$  and  $90^\circ$  respectively.

output to propel the body, we chose a  $83W$  FAULHABER brushed DC motor (with an angle encoder) as Motor 1. Fig. 8 and Fig. 9 show the CAD model and the prototype respectively.

#### IV. EXPERIMENTAL RESULTS

EXO-PANTOE 1 is worn by a subject whose right ankle is injured and can not output sufficient power during walking. With the powered ankle and toe joints, EXO-PANTOE 1 is able to compensate enough energy to the subject and help him relearn the normal walking gait (shown in Fig. 10).

In order to analyze the effects of the segmented foot structure on the energetic efficiency during walking, we have measured the energy consumption of EXO-PANTOE 1 during the subject walking at his most comfortable speed ( $1.1m/s$ ) in three cases. In the first case, the segmented foot of EXO-PANTOE 1 is fixed with a mechanical structure and the foot just acts as a single rigid plate. In the second case, Motor 2 does not work at all and the toe joint can only be bent passively. In the third case, the toe joint is active and it is able to output sufficient net positive work to the subject at TO phase. In these three cases, the ankle joint always provides enough energy to the subject. Before the measurement of the energy consumption in each case, the subject is allowed to have a long enough training period to adapt the exoskeleton.

As shown in Fig. 11, one can find that EXO-PANTOE 1 consumes the most energy in the first case (see Fig. 11(a)), which indicates that the segmented foot plays important role in improving energetic efficiency. The total energy consumed in the second case and the third case is close, where segmented foot with active toe performs slightly better (see Fig. 11(b) and Fig. 11(c)). The ankle joint in the



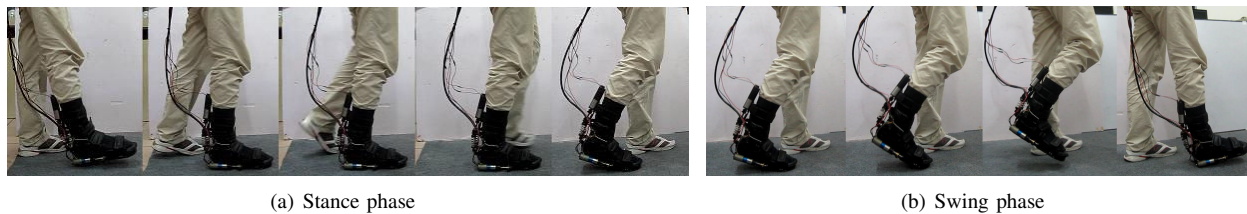


Fig. 10. Sequenced pictures captured from the walking motion of the subject wearing EXO-PANTOE 1 in a walking gait cycle beginning with heel-strike. The result indicates that EXO-PANTOE 1 can assist the subject relearn the human walking gait.

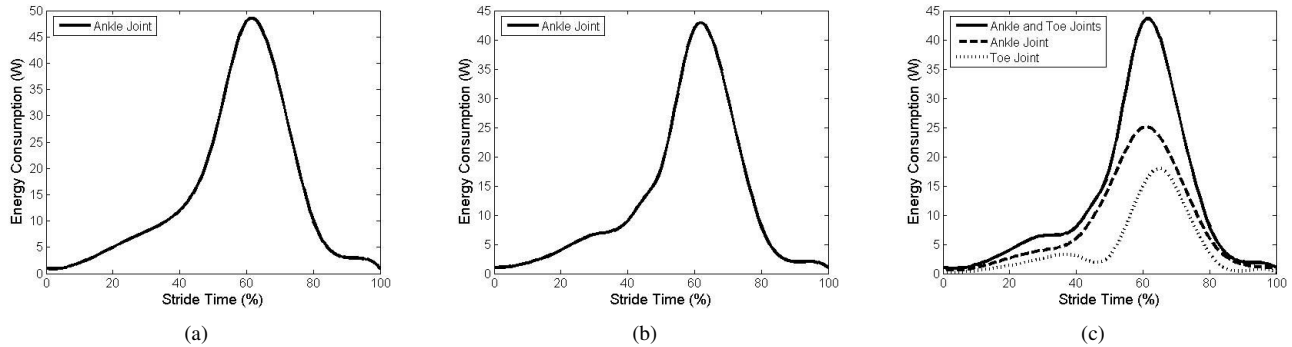


Fig. 11. Energy consumption of EXO-PANTOE 1 in one stride cycle. (a) Energy consumption of EXO-PANTOE 1 when the foot is a single rigid plate. (b) Energy consumption of EXO-PANTOE 1 when the toe joint can only be bent passively. (c) Energy consumption of EXO-PANTOE 1 when the toe joint can output sufficient power.

third case consumes much less energy than that in the second case. The results show that powered toe joint can share the energy cost of the ankle joint. It is helpful to design more efficient and effective powered lower-limb exoskeleton.

## V. CONCLUSIONS AND FUTURE WORKS

In this paper, we have demonstrated the development of EXO-PANTOE 1 with compliant joints and segmented feet. We first proposed a passivity-based dynamic bipedal walking model with segmented feet. The effects of segmented foot structure on walking characteristics were investigated. Simulation results indicates that the segmented foot model with foot structure close to human performs better in energetic efficiency and comparable walking stability compared with rigid foot model. Based on the theoretical analysis, we developed the exoskeleton prototype. Experimental results show that the powered exoskeleton can well assist the subject to relearn the normal walking gaits and the segmented foot structure can well decrease the total energy cost of EXO-PANTOE 1. In future, we will test EXO-PANTOE 1 by measuring the metabolic cost of the subject, and then optimize the control system. In addition, we plan to study EXO-PANTOE 1 on running and stair climbing.

## REFERENCES

- [1] A. M. Dollar, H. Herr, Lower extremity exoskeletons and active orthoses: challenges and state-of-the-art, *IEEE Transactions on Robotics*, vol. 24, no. 1, pp. 144-158, 2008.
- [2] B. R. Fick, J. B. Makinson, Hardiman I prototype, *General Electric Company, Schenectady*, NY, GE Tech. Rep. S-71-1056, 1971.
- [3] A. Chu, H. Kazerooni, A. Zozz, On the biomimetic design of the Berkeley Lower Extremity Exoskeleton (BLEEX), *Proc. of the IEEE International Conference on Robotics and Automation*, pp. 4345-4352, 2005.
- [4] D. P. Ferris, J. M. Czerniecki, B. Hannaford, An Ankle-Foot Orthosis Powered by Artificial Pneumatic Muscles, *Journal of Applied Biomechanics*, Vol. 21, No. 2, pp. 189-197, 2005.
- [5] T. Hayashi, H. Kawamoto, Y. Sankai, Control method of robot suit HAL working as operator's muscle using biological and dynamical information, *Proc. of the IEEE/RSJ International Conference on Intelligent Robots and Systems*, pp. 3063-3068, 2005.
- [6] N. Okita, S. A. Meyers, J. H. Challis, N. A. Sharkey, An objective evaluation of a segmented foot model, *Gait and Posture*, vol. 30, pp. 27-34, 2009.
- [7] M. C. Carson, M. E. Harrington, N. Thompson, J. J. O'Connor, T. N. Theologis, Kinematic analysis of a multi-segment foot model for research and clinical applications: a repeatability analysis, *Journal of Biomechanics*, vol. 34, pp. 1299-1307, 2001.
- [8] B. A. MacWilliams, M. Cowley, D. E. Nicholson, Foot kinematics and kinetics during adolescent gait, *Gait and Posture*, vol. 17, pp. 214-224, 2003.
- [9] K. A. Myers, M. Wang, R. M. Marks, G. F. Harris, Validation of a multisegment foot and ankle kinematic model for pediatric gait, *IEEE Transactions on Neural Systems and Rehabilitation Engineering*, vol. 12, no. 1, pp. 122-130, 2004.
- [10] J. Zhu, Q. Wang, L. Wang, PANTOE 1: Biomechanical design of powered ankle-foot prosthesis with compliant joints and segmented foot, *Proc. of the IEEE/ASME International Conference on Advanced Intelligent Mechatronics*, 2010, pp. 31-36.
- [11] V. T. Inman, H. J. Ralston, F. Todd, *Human Walking*, Baltimore, MD: Williams and Wilking, 1981.
- [12] T. McGeer, Passive dynamic walking, *International Journal of Robotics Research*, vol. 9, pp. 68-82, 1990.
- [13] S. Collins, A. Ruina, R. Tedrake, M. Wisse, Efficient bipedal robots based on passive-dynamic walkers, *Science*, vol. 307, pp. 1082-1085, 2005.
- [14] M. Wisse, A. L. Schwab, F. C. T. Van der Helm, Passive dynamic walking model with upper body, *Robotica*, vol. 22, pp. 681-688, 2004.
- [15] M. Kwan, M. Hubbard, Optimak foot shape for a passive dynamic biped, *Journal of Theoretical Biology*, vol. 248, pp. 331-339, 2007.
- [16] W. J. Wang, R. H. Crompton, Analysis of the human and ape foot during bipedal standing with implications for the evolution of the foot, *Journal of Biomechanics*, vol. 37, pp. 1831-1836, 2004.